Molecular Ecology (2006) **15**, 3601–3615 doi: 10.1111/j.1365-294X.2006.03046.x

Genetics of recent habitat contraction and reduction in population size: does isolation by distance matter?

RAPHAEL LEBLOIS,*†‡ ARNAUD ESTOUP† and REJANE STREIFF†
Laboratoire Génétique et Environnement, CNRS-UMR 5554, 34095 Montpellier, France, †Centre de Biologie et de Gestion des Populations, INRA, Campus International de Baillarguet, CS 30016, 34988 Montferrier sur Lez cedex, France

Abstract

Fragmentation and loss of natural habitats are recognized as major threats to contemporary flora and fauna. Detecting past or current reductions in population size is therefore a major aim in conservation genetics. Statistical methods developed to this purpose have tended to ignore the effects of spatial population structure. However in many species, individual dispersal is restricted in space and fine-scale spatial structure such as isolation by distance (IBD) is commonly observed in continuous populations. Using a simulation-based approach, we investigated how comparative and single-point methods, traditionally used in a Wright–Fisher (WF) population context for detecting population size reduction, behave for IBD populations. We found that a complex 'quartet' of factors was acting that includes restricted dispersal, population size (i.e. habitat size), demographic history, and sampling scale. After habitat reduction, IBD populations were characterized by a stronger inertia in the loss of genetic diversity than WF populations. This inertia increases with the strength of IBD, and decreases when the sampling scale increases. Depending on the method used to detect a population size reduction, a local sampling can be more informative than a sample scaled to habitat size or vice versa. However, IBD structure led in numerous cases to incorrect inferences on population demographic history. The reanalysis of a real microsatellite data set of skink populations from fragmented and intact rainforest habitats confirmed most of our simulation results.

Keywords: bottleneck, habitat reduction, isolation by distance, limited dispersal, summary statistics

Received 14 February 2006; revision accepted 2 June 2006

Introduction

Fragmentation and loss of natural habitats caused by human activities and changes in land use are recognized as major threats to contemporary flora and fauna (Diamond 1989; Saunders *et al*. 1991; Fahrig 2003; Stockwell *et al*. 2003). A combination of demographic, environmental and genetic effects may lead to population extinctions, but the relative impact of each factor and their potential interactions remain the subject of research and debate (Lande 1988; Lacy & Lindenmayer 1995; Oostermeijer *et al*. 2003). It is admitted, however, that habitat fragmentation will increase genetic drift by reducing both gene flow among populations and population size in small remnant fragments (Frankel & Soulé 1981; Young & Clarke 2000; Stockwell *et al*. 2003). Inferring population size decline has thus become increasingly important in population genetics, especially in a conservation biology context.

A large reduction in population size increases rate of inbreeding, loss of genetic variation, fixation of deleterious alleles, and thereby greatly reduces adaptive potential and increases risk of extinction (Frankel & Soulé 1981; Lande 1988; Dunham *et al*. 1999; Dudash & Fenster 2000). In natural populations, the level of genetic diversity is generally measured at evolutionary neutral loci through heterozygosity and number of alleles. Although the link between those statistics and extinction risks is not straightforward, a few recent studies have shown negative correlations between individual heterozygosity and extinction risk in butterflies, *drosophila* and mice (Hedrick & Kalinowski 2000 and references therein). Variation at neutral genetic markers

Correspondence: Réjane Streiff, Fax: (33) 4 99 62 33 45; E-mail: streiff@ensam.inra.fr
‡Present address: University of California, Department of Integrative Biology, Berkeley, California 94720-3140, USA.

is also widely used for inferring demographic fluctuations (Beaumont 1999; Goldstein & Harvey 1999; Goldstein *et al*. 1999; Beaumont 2004). This is because surveys based on molecular screening are often more practical than ecological or demographic studies entailing long-term population surveys. In this case, characterizing genetic diversity in fragmented landscape aims at making inferences on demographic trends and parameters that are useful for *in situ* or *ex situ* management strategy, rather than on extinction risk (McGlaughlin *et al*. 2002; Hurt & Hedrick 2004; Wayne & Morin 2004).

Depending on the biological context and data available, two categories of approaches have traditionally been applied to evaluate the impact of fragmentation and demographic fluctuations on genetic diversity. *Comparative approaches* are based on the comparison of various summary statistics of genetic variation measured in several populations (using a single data set per population), among which one or several populations are considered as a 'control', because independent sources of information indicate past demographic stability for these populations (Gaines *et al*. 1997; Williams *et al*. 2003; Sumner *et al*. 2004). A similar approach consists of comparing genetic diversity values measured in data sets collected at different points in time in a single population, for example, before and after hypothetical demographic fluctuations (Queney *et al*. 2000; Guinand & Scribner 2003; Miller & Waits 2003).

In practice, such comparative approaches may be difficult to carry out because such controls are scarcely available (especially in time), or due to the difficulty to clearly identify anthropogenically fragmented habitats (Fahrig 2003). *Single-point approaches* have thus been developed to detect demographic fluctuations, especially population size reductions through bottlenecks, using genetic data from a single population sample (i.e. without a control). In these single-point approaches, the detection and intensity estimation of a bottleneck are based on maximum-likelihood methods (e.g. Griffiths & Tavaré 1994; Kuhner *et al*. 1998; Beaumont 1999), or on assessment of deviations from expected mutation-drift values of various statistics, such as the number of alleles, the heterozygosity, or the distribution of alleles in a sample (e.g. Cornuet & Luikart 1996; Reich & Goldstein 1998; Garza & Williamson 2001).

All single-point approaches are based on simple demographic models, especially on the classic Wright–Fisher (WF) model of a closed panmictic population (WF; Fisher 1921, Wright 1931). However, in numerous species, individual dispersal is restricted in space. This means that there is a higher probability that individuals mate with individuals born in close proximity to themselves than individuals born far away. Empirical studies on animals and plants have repeatedly demonstrated such restricted dispersal (e.g. for plant data, see Crawford 1984; Fenster *et al*. 2003; Vekemans & Hardy 2004; for animal data, see Endler 1977; Rousset 1997, 2000; Spong & Creel 2001; Sumner *et al*. 2001). Initially introduced by Wright (1943, 1946), isolation-by-distance (IBD) models take into account this biological feature. Reduction of habitat surface leads to a reduction in the number of individuals within both a WF and a continuous IBD population. Hence, it is tempting, at least from a demographic point of view, to parallel habitat reduction in a continuous IBD population to a reduction in population size in a WF population (i.e. a bottleneck). However, standard population genetics statistics may behave differently under each population model, leading to biased inferences of demographic and evolutionary processes if spatial population structure is ignored. In agreement with this, computer simulations and empirical data have shown a substantial effect of spatial population structure and sampling scale on Tajima's *D* statistics (Tajima 1989), leading to potential false detection of past demographic expansion (Ptak & Przeworski 2002; Pannell 2003). However, these studies focused on a single statistic (Tajima's *D*) designed for the detection of ancient population growth using sequence data and considered simple (and hence potentially unrealistic) models of migration.

A few theoretical studies have analysed more realistic population models such as isolation-by-distance models (Malécot 1948; Wright 1951; Maruyama 1972; Barton & Wilson 1995; Rousset 1997, 2004). They show that: (i) IBD populations of small size can be regarded as panmictic populations unless dispersal is 'strongly restricted' in space. Determining the threshold value of the dispersal parameters below which the panmictic approximation does not hold anymore, however, remains controversial (see Maruyama 1972 and Kawata 1995); (ii) the decay of observed heterozygosity in an equilibrium population is strongly dependant on dispersal rates but also on the shape of the dispersal distribution (Maruyama 1972; Barton & Wilson 1995; Rousset 2004). It is worth stressing that all those studies focused on a single statistic, namely the observed heterozygosity, and considered only populations at mutation-drift–migration equilibrium. This is mainly because, contrarily to the WF and island models (e.g. Crow & Kimura 1970), analytical treatment of coalescence time or coalescence probabilities are not available for more than two genes under IBD models (e.g. Wilkins 2004), even for equilibrium situations. Therefore, in continuous IBD populations, no analytical treatment can be used to derive a relationship between various standard population genetics statistics (except the heterozygosity) and population sizes; *a fortiori* when one wants to assess the behaviour of those statistics after a reduction in population size due to habitat contraction.

In this study, we used a simulation-based approach to assess the influence of IBD structure on the detection of population size reduction due to habitat reduction. Such effects were assessed using some of the comparative and single-point approaches mentioned above. Referring more

specifically to microsatellite markers, we assessed the influence of IBD structure on: (i) the variation of standard genetic diversity measures (heterozygosity and number of alleles) after a reduction in habitat surface; and (ii) the probability of detecting population size reduction using two commonly used single-point approaches (i.e. those of Cornuet & Luikart 1996; Garza & Williamson 2001). Finally, we have illustrated our simulation-based results with a real microsatellite data set obtained for several skink populations collected in fragmented and intact rainforest habitats (Sumner *et al*. 2004, 2001). The populations of this species are characterized by IBD structure at a local scale, and the habitat fragmentation history is well documented, hence allowing pertinent comparisons with our simulation-based results.

Models and methods

Demographic models and population cycle

The model that we considered for continuous populations under IBD is the lattice model with each lattice node corresponding to one diploid individual. This model without demic structure is viewed as an approximation for truly continuous populations with infinitely strong density regulation (i.e. density is fixed in time and space so that migration is not density-dependant and individuals are not clustering; Malécot 1975; Rousset 2000). In those models, the term population is used to designate the total number of individuals in the entire habitat. To avoid edge effects, a two-dimensional lattice is usually represented on a torus (e.g. Rousset 2000; Leblois *et al*. 2003, 2004). However, because small populations and hence small lattices were also considered here, a representation on a torus was inappropriate. Therefore, we considered a two-dimensional lattice represented on a plane with reflective edges (i.e. gametes come back to the system when they disperse further than the boundaries, as the light in a mirror) or absorbing edges (i.e. gametes are lost from the system when they disperse farther than the boundaries). For all the parameter ranges considered in this study, reflective and absorbing edges gave similar results (results not shown). Hence, only results obtained using reflective boundaries were further detailed. For comparison, a WF population model without any substructure was also considered (Fisher 1921; Wright 1931).

For all simulations, generations are discrete and the life cycle is divided into five steps: (i) at each reproductive event, each individual gives birth to a great number of gametes, and dies; (ii) gametes undergo the effect of mutations; (iii) gametes disperse (only for IBD models); (iv) diploid individuals are formed; and (v) competition brings back the number of adults at each node to N, with $N = 1$ for the IBD models and N is the size of the whole population for the WF model. We assume here random assortment of gametes after dispersal at each node.

Coalescent algorithm

Because of the complexity of the IBD models considered, the coalescent algorithm used in this study is not based on the large-N approximation of the n-coalescent theory (Kingman 1982a, b; Nordborg 2001). It is an exact algorithm for which coalescence and migration events are considered generation by generation up to the common ancestor of the sample. The idea of tracing lineages back in time, generation by generation, is fundamental in the coalescence theory, and is well described in Nordborg (2001). Such a generation by generation algorithm leads to less efficient simulations in terms of computation time than those based on the n-coalescent theory. However, this algorithm is much more flexible when complex demographic and dispersal features are considered. The generation-by-generation algorithm that gives the coalescent tree for a sample of n genes evolving under IBD has been detailed in Leblois *et al*. (2003, 2004).

Dispersal functions in IBD models

Biologically realistic dispersal functions often have a high kurtosis (Endler 1977; Kot *et al*. 1996). The commonly used discrete probability distributions for dispersal are not appropriate here because high kurtosis can be achieved only by assuming a low dispersal probability (i.e. that most offspring reproduce exactly where their parents reproduced; Rousset 2000). Thus, we used dispersal distributions for which the probability of moving k steps (for $0 < k \leq K_{max}$) on one line is of the form $f_k = f_{-k} = M/k^n$, with parameters M and n, controlling the total dispersal rate and the kurtosis, respectively, and k and $-k$ referring to both possible directions of dispersal on the given line, so that the dispersal is assumed to be symmetric. By suitable choice of M and n parameter values, large kurtosis can be obtained with high migration rates (Rousset 2000). Dispersal was assumed to be independent in each direction, so that $f_{dx,dy} = f_{dx} \times f_{dy}$.

Three dispersal distributions were used to simulate IBD populations with three levels of limited dispersal. For the first dispersal distribution considered, $M = 0.555$ and $n = 2.744$ for $0 < k \leq 48$, so that the second moment of this distribution, i.e. the mean squared parent–offspring distance, is equal to four lattice units ($\sigma^2 = 4$). The second dispersal distribution ($M = 0.547$ and $n = 3.798$ for $0 < k \leq 48$), corresponds to a more limited dispersal, with $\sigma^2 = 1$ lattice unit. The third dispersal distribution is a simple stepping stone dispersal scheme with a migration rate for adjacent lattice nodes $f_1 = f_{-1} = 1/6$ and a null migration rate for all pairs of nonadjacent nodes. It is the strongest IBD model considered in this study: in this case $\sigma^2 = 1/3$. The three dispersal distributions described above correspond to relatively strong isolation-by-distance situations, which however, appear biologically reasonable for many species (see References cited in Introduction). Simulations with $\sigma^2 = 20$ gave results

Table 1 Models and sampling design used to study the effects of IBD structure on the detection of population size reduction

		Population sizes: no. of individuals (in lattice node sizes for IBD)				
		From sampling time to G_c	From G_c to the TMRCA	Reduction factor	Local sampling (in lattice node)	Scaled sampling (in lattice node)
Nonequilibrium populations	Small populations	49 (7×7)	4900 (70×70)	100	(6×5)	NC
	Medium size populations	100 (10×10)	10 000 (100×100)	100	(6×5)	NC
	Large populations	400 (20×20)	40 000 (200×200)	100	(6×5)	(18×15)
Equilibrium populations		400 (20×20)		NA	(6×5)	(18×15)
		1600 (40×40)		NA	(6×5)	(36×30)
		4900 (70×70)		NA	(6×5)	(66×55)
		10 000 (100×100)		NA	(6×5)	(96×80)
		40 000 (200×200)		NA	(6×5)	(198×165)
		160 000 (400×400)		NA	(6×5)	(396×330)

The number of generations, G_c, indicates the moment in the past when the population size reduction occurred. TMRCA corresponds to the time of the most recent common ancestor of the sampled genes. IBD, isolation by distance; NC, not considered, NA, not appropriate

close to those obtained for WF populations (results not shown), indicating that all results presented below only concern species with considerably limited dispersal abilities (i.e. $\sigma^2 << 20$). Because the density D is always one individual per lattice node, the value σ^2 will further be used to characterize the strength of IBD structure in our simulations. Note that the WF population model considered in this study can be interpreted as a nonlimited uniform dispersal with an infinite second moment of dispersal.

Mutation processes

Mutations were added on each branch of the coalescent tree considering a binomial distribution with parameter (μ, L), where μ is the mutation rate and L the length of the branch. Microsatellite markers were simulated in the present study. The generalized stepwise model (GSM) in which the change in the number of repeat units forms a geometric random variable was adopted (Pritchard *et al*. 1999; Estoup *et al*. 2001). Even if the GSM does not capture all the complexity of the mutation process at microsatellite loci (reviewed in Ellegren 2000; Schlotterer 2000), this model is more realistic than the traditional stepwise mutation model (SMM, Ohta & Kimura 1973). In the GSM, the change in the number of repeat units formed a geometric distribution with a variance equal to 0.36 (Estoup *et al*. 2001). Mutation rate was equal to 5×10^{-4} for all loci, a value considered as the average mutation rate in many species (reviewed in Estoup & Angers 1998).

Reduction of habitat surface

Our simulations focused on the reduction of habitat surface with constant density of individuals (Fig. 1). The population surface reduction occurred at generation G_c in the past and was instantaneous; the population went in a single generation from an initial surface S_i with N_i individuals to a final surface S_f with N_f individuals. The position of the surface after reduction is randomly chosen on the initial population grid (Fig. 1). Note that this model also describes the case of a single population fragment which becomes isolated from the main population as a result of habitat fragmentation. Three different population size settings were studied, from a small N_f value of 49 diploid individuals to a larger N_f value of 400 diploid individuals; in all cases a constant bottleneck factor (N_i/N_f) of 100 was applied, so that initial population sizes (N_i) varied from 4900 to 40 000 (see Table 1 for details). Because this study refers to fragmentation and loss of natural habitats caused by human activities, only recent habitat surface reductions were simulated. Hence, for each population size setting, four

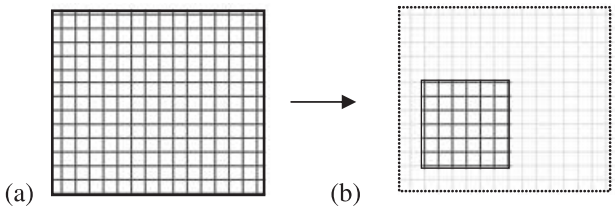

Fig. 1 Schema of a habitat/population size reduction with constant density as modelled in this study for IBD models. The grid (a) corresponds to population before habitat reduction. The grid (b) corresponds to the remnant habitat of the population after its spatial reduction (black grid). The ancient habitat surface is indicated in light grey grid. The habitat reduction occurs in a single generation and the position of the population (i.e. the remnant habitat) after reduction is randomly located on the light grey grid.

simulations were run with G_c = 20, 100, 200 generations, and G_c = 0 (i.e. no habitat reduction) as baseline for mutation-drift–migration equilibrium.

Sampling design

Each simulation run provides genotypes at 10 independent polymorphic loci for 30 diploid individuals. These sample sizes were considered as representative of the number of loci and individuals commonly analysed in empirical studies based on microsatellites. Note that preliminary simulations considering a sample size of 100 individuals showed similar results (results not shown). Independent coalescent trees were used to simulate multilocus genotypes at independent loci. This process was repeated 1000 times giving 1000 multilocus samples of 30 diploid individuals sharing the same demographic history. For simulations of IBD populations, individuals characterized by their coordinates on the lattice were sampled regularly on a squared area. Two extreme sampling scales have been considered: a local sample corresponding to 30 individuals located on each adjacent node of a (6×5) node lattice area located in the middle of the remnant population, and a scaled sample including 30 individuals located on the entire surface of the remnant population. For instance, a scaled sample included one individual every three or 33 nodes for a continuous population of 400 or 40 000 individuals, respectively (see Table 1). Note that, because of too small surfaces, only local samples were considered for IBD populations with less than 400 individuals. In WF populations, sampled individuals were obviously not georeferenced.

Summary statistics and methods investigated

For each simulated sample, two standard summary statistics were computed and averaged over the 10 loci: the so-called gene diversity or expected heterozygosity, $H_E = n/(n-1)(1 - \sum_i p_i^2)$, where p_i is the frequency of allele i and n the gene sample size (Nei 1987), and the observed number of alleles in the sample, A. Because it often appears in mathematical analysis of population genetic models, we also computed the observed individual heterozygosity $H_O = (1 - Q_0)$, where Q_0 is the probability of identity in state of two genes taken in the same individual. Two additional statistics used in the single-point methods for detecting population size reduction from microsatellite data, published by Cornuet & Luikart (1996) and Garza & Williamson (2001), were computed: (i) ΔH, the difference between the gene diversity H_E computed from the gene sample and H_A the heterozygosity expected from the observed number of alleles in the gene sample for an equilibrium WF population (Cornuet & Luikart 1996); and (ii) $M = \sum_{l=1}^{L} k_l / \sum_{l=1}^{L} (1 + r_l)$, where k_l is the number of alleles at the l-th locus, r_l is the difference in number of repeats between the largest and the smallest allele at locus l (i.e. the range of allele sizes), and L is the number of loci (Garza & Williamson 2001).

The basic principles underlying the behaviour of ΔH and M statistics in a population size reduction context are the following: (i) ΔH is expected to take positive values after a population size reduction (i.e. heterozygosity excess), because allelic diversity is reduced faster than gene diversity (Nei *et al*. 1975; Cornuet & Luikart 1996). At mutation-drift equilibrium, ΔH should be equal to zero; (ii) M is expected to decrease after a population size reduction because the range in allele size at a locus (denominator) decreases more slowly than the number of alleles (numerator) under genetic drift. This latter assumption is based on the empirical assessment that the shortest and longest alleles at a microsatellite locus are usually not the rarest. As allelic loss through genetic drift is inversely correlated to the allele frequencies, the range in allele size should remain roughly stable, whereas alleles intermediate in size will disappear. Garza & Williamson (2001) have shown through empirical and simulated data that M-values were greater than 0.68 in WF populations at mutation-drift equilibrium.

To further investigate the behaviour of the single-point method of Cornuet & Luikart (1996), we analysed a subset of 100 simulated samples for each studied case using the version 1.2.02 of the software BOTTLENECK (Piry *et al*. 1999). These analyses were performed assuming both the SMM as conservative mutation model for the detection of population size reduction (Cornuet & Luikart 1996) and a GSM with a geometric variance of 0.36 (cf. same mutational model as for our simulated microsatellite data). For each simulated sample, a Wilcoxon signed rank test was used to test for a significant heterozygosity excess (i.e. $P < 0.05$), the latter deviation usually being considered as a signal of population size reduction (e.g. Cornuet & Luikart 1996; Luikart & Cornuet 1998).

Results

Populations at equilibrium

Figure 2 presents the number of alleles (A), the gene diversity (H_E) and the observed heterozygosity (H_O) for WF populations and IBD populations with different σ^2 values at equilibrium (i.e. with constant habitat/population size). For IBD populations, results are given for both local samples and samples scaled to the habitat size. For local samples, lower values of A, H_E and H_O were obtained for IBD populations than for WF populations with equivalent sizes. The differences between WF and IBD models increase with the strength of IBD (low σ^2 values). Note that, although the variations of H_E and H_O with population size were qualitatively similar, H_O was more affected by IBD structure than H_E (Fig. 2b, c). For all statistics, the differences between population models become negligible for small population

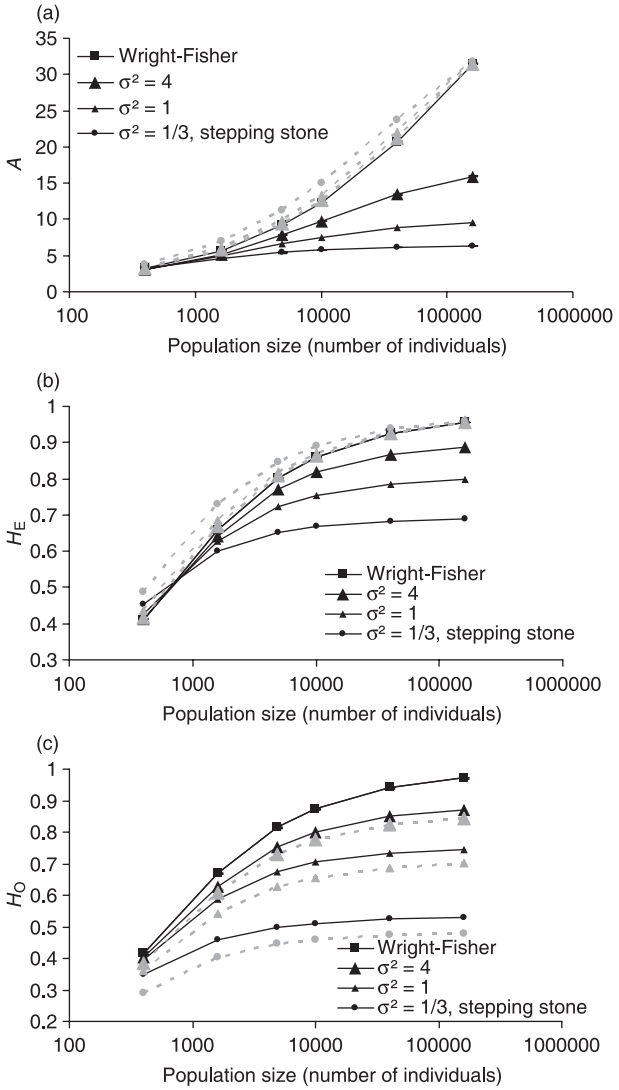

Fig. 2 Number of alleles and heterozygosity in equilibrium population. (a) Number of alleles (A), (b) Expected heterozygosity (H_E) and (c) Observed heterozygosity (H_O) as a function of population size and model considered. Black curves are for local samples and grey dotted curves are for scaled samples. Note that the x-axis scale is logarithmic.

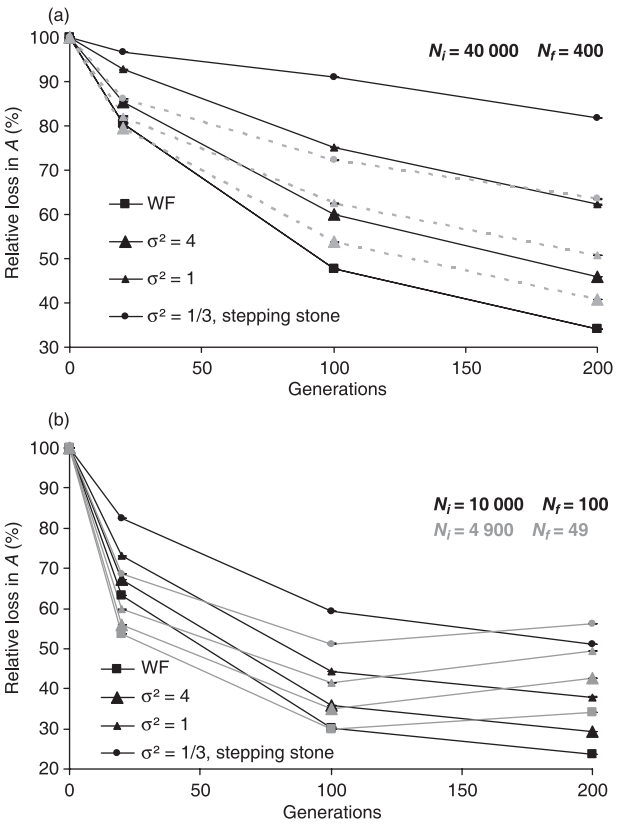

Fig. 3 Loss in allele number after a habitat reduction. Relative loss in allele number (A) for a local sample (plain curves) is represented as a function of time after habitat reduction for different population models. (a) Large population sizes of 400 individuals after reduction and 40 000 before; (b) Plain black curves: medium population sizes of 100 individuals after reduction and 10 000 before; Plain grey curves: small population sizes of 49 individuals after reduction and 4900 before. In (a) grey dotted curves represent the relative loss in A for a scaled sample.

sizes; for instance A, H_E, and H_O values are similar for a population of 400 individuals whatever the population model.

The effect of the sampling scale is similar for A and H_E, but different for H_O (Fig. 2). In IBD populations, A and H_E values are considerably higher in scaled samples than in local samples. They are also slightly higher than those in WF populations, especially for strongly structured IBD populations (e.g. $\sigma^2 = 1/3$). By contrast, H_O values are lower when computed from a scaled sample than from a local sample, and hence remain considerably lower than under a WF model (Fig. 2c).

Habitat reduction: comparative approach

The relative losses of A and H_E after a habitat contraction [i.e. $(A_{equilibrium} - A_{after\ reduction})/A_{equilibrium}$ and $(H_{equilibrium} - H_{after\ reduction})/H_{equilibrium}$] are shown in Figs 3 and 4, respectively. As expected, A decreases more quickly than H_E in a WF population (Nei *et al*. 1975; Cornuet & Luikart 1996). This trend also holds for IBD populations, but the relative loss of both A and H_E was found to be lower than for WF populations, especially for a local sample. This lower relative loss is particularly pronounced for large final population size and strongly limited dispersal. For a stepping stone population ($\sigma^2 = 1/3$) with $N_f = 400$, the relative allele number is still > 90%, 100 generations after the habitat reduction, whereas it is only 50% in a WF population. The difference of loss between IBD and WF populations is less important for H_E than for A (e.g. 97% vs.

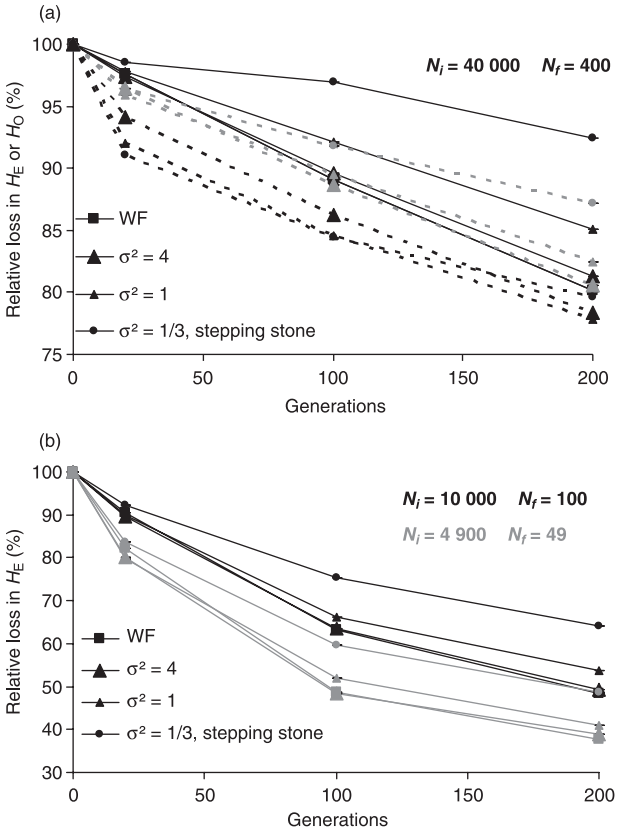

Fig. 4 Loss in heterozygosity after a habitat reduction. Relative loss in expected heterozygosity (H_E) for a local sample (plain curves) is represented as a function of time after habitat reduction for different demographic models (see legend of Fig. 3 for the (a) and (b) cases). In (a) dotted curves represent the relative loss in H_E (grey curves) and the relative loss in H_O (black curves) for a scaled sample.

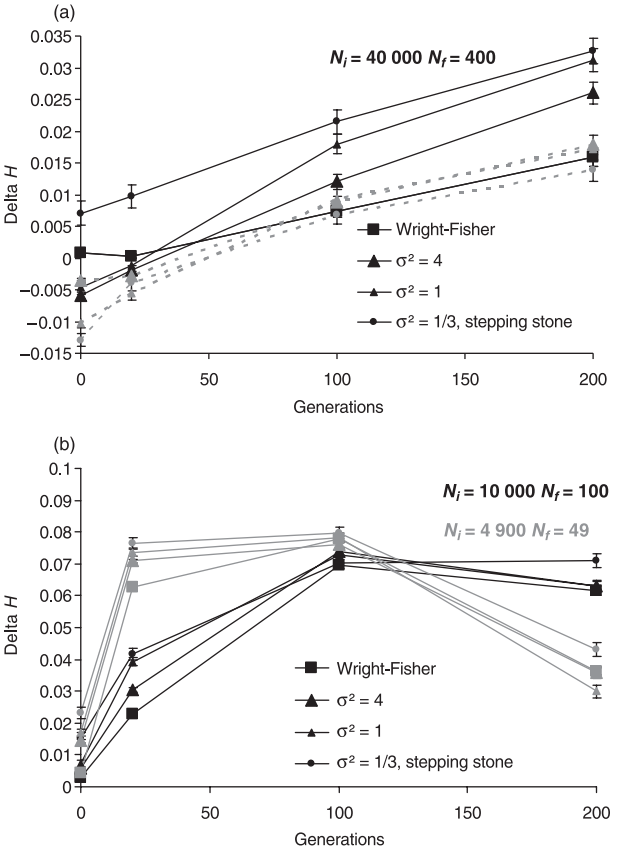

Fig. 5 Effect of habitat reduction on the statistics ΔH. The statistics ΔH (Cornuet & Luikart 1996) computed for a local sample (plain curves) is represented as a function of time after habitat reduction and different population models (see legend of Fig. 3 for the (a) and (b) cases). In (a) the grey dotted curves represent ΔH for a scaled sample.

89% when referring to the previous situation). In all studied cases, the differences between IBD and WF populations reduce when the strength of IBD structure decreases (i.e. when σ^2 increases). Results for H_O for a local sample are similar to those for H_E (results not shown).

Figures 3a and 4a show that using a scaled sample instead of a local sample reveals larger differences in A and H_E between equilibrium and size reduced IBD populations. While for A such differences remain smaller than in a WF population, the decrease in H_E is slightly faster in IBD population than in WF populations for recent habitat reduction (e.g. 20 generations after the reduction; Fig. 4a). It then becomes slower for IBD populations with older habitat reductions (e.g. after 100–200 generations). A faster decrease in H_O computed from a scaled sample in IBD populations than in WF populations is also observed for recent habitat reductions, and this decrease is stronger for H_O than for H_E (Fig. 4a).

Habitat reduction: single-point approach of Cornuet & Luikart (1996)

Figure 5 shows that, as expected, the statistic ΔH takes null or slightly positive values for WF populations at equilibrium. For local samples, mean ΔH values for equilibrium IBD populations are relatively similar to those for equilibrium WF populations; they are slightly positive or negative depending on the case studied (i.e. from $\Delta H = -0.006$ for $N_i = 40\,000$ and $\sigma^2 = 4$ to $\Delta H = 0.023$ for $N_i = 4900$ and $\sigma^2 = 1/3$).

After the population size reduction, ΔH variation shows a similar pattern for WF and IBD models, and this for all N_f values studied (note the y-scale in Fig. 5a). ΔH values increase with time since population size reduction, often at a slightly greater rate in IBD than in WF populations. Although the time intervals we used are too large to have a precise distribution of ΔH over time, our results support previous observations from Cornuet & Luikart (1996) by

showing that maximum ΔH values are reached after around N_f generations for both population models, and then decrease (our simulation time window is too short to observe the maximum ΔH values for $N_f = 400$). A larger scaled sample reduces the differences between population models of ΔH variation after population size reduction (Fig. 5a). However, increasing the sampling scale also tends to produce larger negative ΔH values in equilibrium IBD populations, which are still observed in the generations immediately following population size reduction (e.g. 20 generations).

The behaviour of the single-point method of Cornuet & Luikart (1996) was further investigated by computing, with the software BOTTLENECK (Piry *et al*. 1999), the proportion of significant excess of heterozygosity (usually interpreted as a population size reduction) in a subset of 100 simulated data sets for each combination of parameters. Our results, presented in Fig. 6, first illustrate the low power of the method (at least for a reduced number of loci, i.e. 10) in getting a significant signal of population size reduction when a conservative SMM is assumed for markers, and this whatever the population model (at best 25% of population size reduction detected; Fig. 6c). The power considerably increases when considering the actual GSM mutation model (up to 60%; Fig. 6c). However, a non-negligible bias could be observed in this case, with 1 to 22% significant excess of heterozygosity detected in equilibrium populations.

Interestingly, while IBD structure has little effect on the proportion of significant population size reduction signals detected, it has a strong effect on the detection of false signals of population expansion (i.e. negative ΔH values corresponding to a deficit of heterozygosity). In the case of equilibrium or recently bottlenecked IBD populations, the method detects significant signals of population expansion in up to 34% of the data sets when a local sample is considered and an SMM is assumed (Fig. 7). This false expansion detection rate increases with the strength of IBD, the size of the population and the scale of the sample (i.e. up to 48%, Fig. 7c). This bias has been confirmed by simulations of IBD populations with $N_f = 1600$ individuals, for which the proportion of false expansion detection reached 57% for a local sampling strategy and up to 70% for a large sampling scale (results not shown). Proportion of false expansion, however, decreases with the number of generations after the population size reduction. Moreover it is considerably lower when the actual GSM mutation model is assumed, although reaching 18% for large population size with strong IBD structure (Fig. 7c).

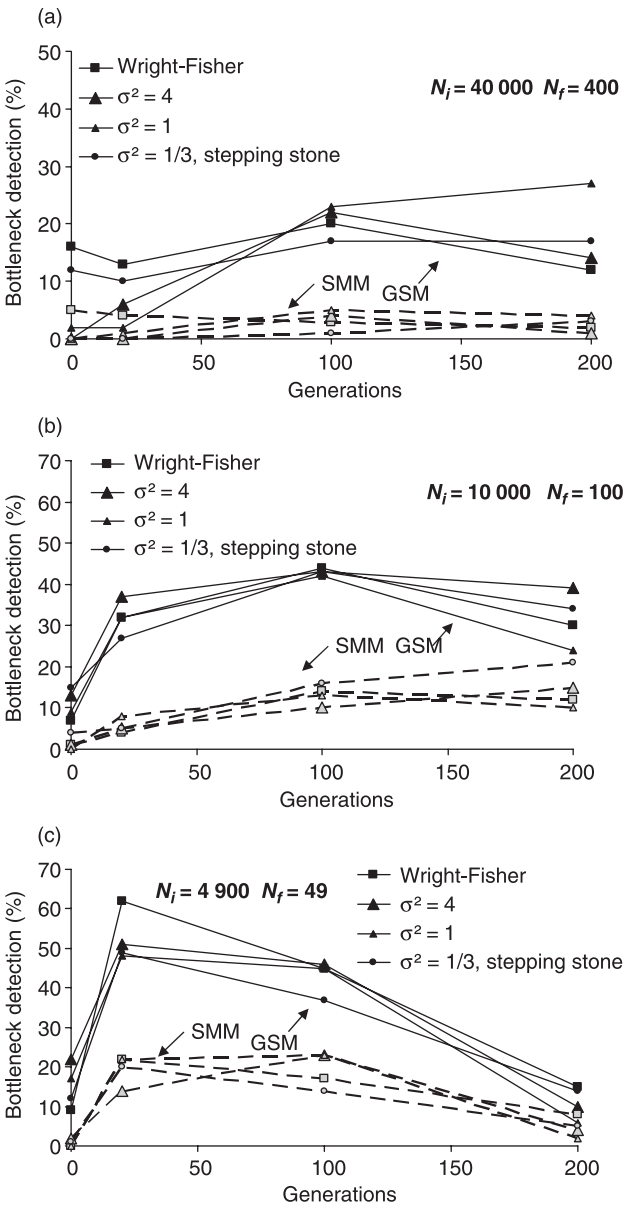

Fig. 6 Detection of population size reduction using the software BOTTLENECK. The proportion of significant (i.e. Wilcoxon signed rank test; $P < 0.05$) population size reduction detected on a subset of 100 simulations is represented as a function of time after habitat reduction and different population models. (a) large population sizes of 400 individuals after reduction and 40 000 before; (b) medium population sizes of 100 individuals after reduction and 10 000 before; (c) small population sizes of 49 individuals after reduction and 4900 before. Dotted curves with grey motifs correspond to analysis assuming the SMM and black curves with black motifs correspond to analyses computed assuming the GSM with variance equal to 0.36.

Habitat reduction: single-point approach of Garza & Williamson (2001)

In agreement with Garza & Williamson (2001), Figure 8 shows that for WF populations and mutation models realistic for microsatellite loci, a value of $M < 0.68$ indicates a recent reduction in population size. On the other hand, equilibrium M-values are strongly influenced by IBD structure, and decrease with increasing strength of IBD

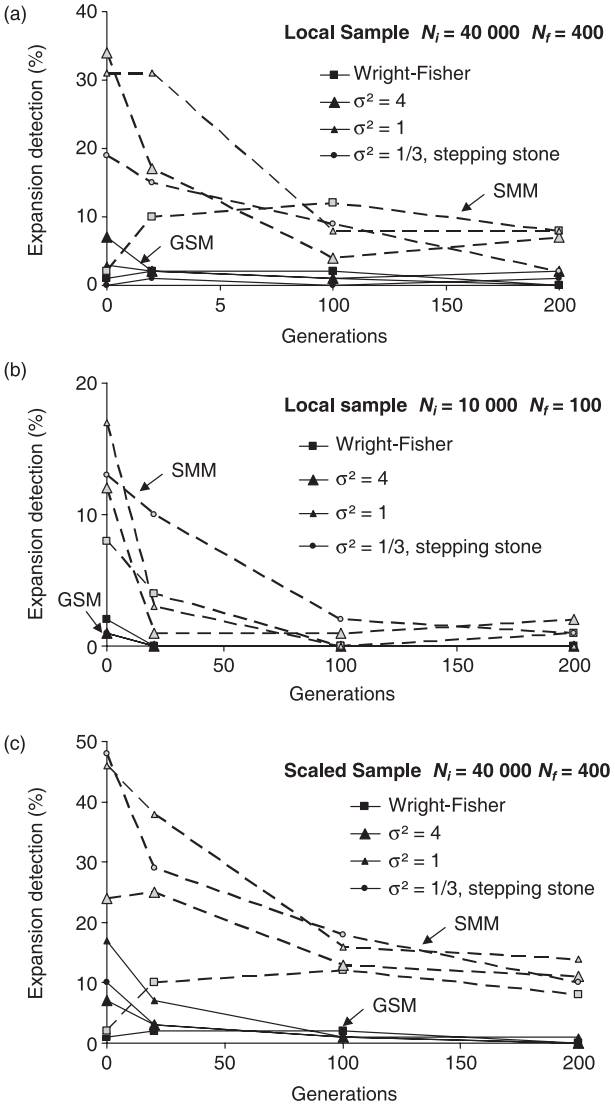

Fig. 7 False population expansion detected using the software BOTTLENECK. The proportion of false expansion signal (i.e. significant deficit in heterozygosity; Wilcoxon signed rank test, $P < 0.05$) from a subset of 100 simulations is represented as a function of time after habitat reduction and for different population models. (a) large population sizes of 400 individuals after reduction and 40 000 before with a local sample, (b) medium population sizes of 100 individuals after reduction and 10 000 before with a local sample, (c) large population of 400 individuals after reduction and 40 000 before with a scaled sample. Dotted curves with grey motifs correspond to analysis assuming the SMM and black curves with black motifs correspond to analyses computed assuming the GSM with variance equal to 0.36.

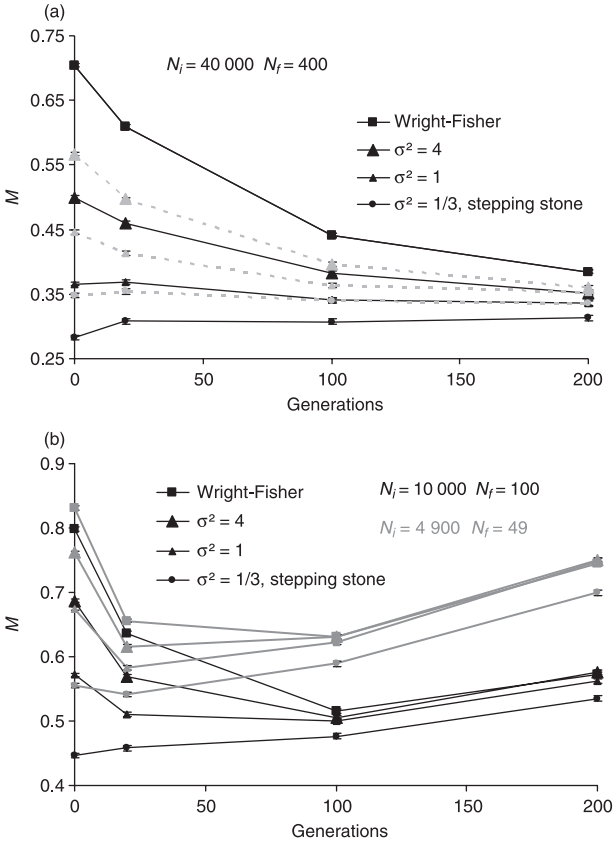

Fig. 8 Effect of habitat reduction on the statistics *M*. The statistics *M* computed from a local sample (plain curves) is represented as a function of time after habitat reduction and for different population models (see legend of Fig. 3 for the (a) and (b) cases). In (a) the dotted grey curves represent *M* for a scaled sample.

(see *M*-values at generation zero in Fig. 8a and b). In most cases studied, IBD equilibrium *M*-values are lower than the critical value of 0.68 proposed by Garza & Williamson (2001).

The behaviour of the *M* statistic after a habitat reduction depends on the strength of IBD. *M*-values usually decrease after habitat reduction, but to a lower extent than in WF populations. They also remain lower than equilibrium values during a shorter time span than in WF populations, and then become larger than initial equilibrium values. This is because equilibrium *M*-values are larger in IBD populations of smaller size than before habitat reduction (Fig. 8b). For strongly limited dispersal (i.e. $\sigma^2 = 1/3$), the time window during which *M*-values are lower than initial equilibrium values are probably too short to be visualized, so that *M*-values appear to increase immediately after the habitat reduction. Computing *M*-values from a (larger) scaled sample does not change all above observations (Fig. 8a).

Illustration from real data

Sumner *et al*. (2001) have shown, using both demographic and genetic methods based on individual genotypes at nine

Table 2 Summary of skink population data set

Population name	Type	Area	Size	No.	A	H_E	H_O	M	Bot P value		Exp P value	
									SMM	GSM	SMM	GSM
Souita Falls (F1)	F	2.0	101–384	25	7.35	0.70	0.68	0.458	0.99	0.85	0.007**	0.18
Maalan Road (F2)	F	2.46	124–472	42	7.44	0.63	0.66	0.549	1.00	0.99	0.001**	0.01**
Waltham (F3)	F	2.64	133–507	27	7.75	0.68	0.67	0.496	0.99	0.90	0.007**	0.13
Pat Daley Park (F4)	F	5.96	300–1144	18	7.39	0.63	0.63	0.406	1.00	0.99	0.002**	0.01**
Nose Ring (F5)	F	24.19	1217–4645	29	9.31	0.70	0.68	0.524	1.00	0.99	0.005**	0.007**
Whiteing Road (F6)	F	36.31	1826–6972	30	8.77	0.71	0.69	0.522	1.00	0.99	0.005**	0.01**
Millaa Millaa Falls (F7)	F	65.06	3273–12497	27	7.88	0.66	0.65	0.465	1.00	1.00	0.001**	0.003**
Brotherton(C1)	C	NA	>> 40 000	28	8.26	0.69	0.68	0.523	0.99	0.98	0.019**	0.065
Cross-eye(C2)	C	NA	>> 40 000	30	8.00	0.69	0.70	0.526	1.00	1.00	0.001**	0.005**
Mount Father Clancy(C3)	C	NA	>> 40 000	32	8.77	0.69	0.72	0.575	1.00	1.00	0.002**	0.005**
Reynolds(C4)	C	NA	>> 40 000	28	9.18	0.66	0.71	0.566	1.00	1.00	0.002**	0.002**
Massey Creek(C5)	C	NA	>> 40 000	94	7.95	0.62	0.62	0.580	1.00	1.00	0.001**	0.002**

For each population, habitat type (F, fragmented and C, continuous, i.e. nonfragmented) is reported, as well as its surface (in ha, for fragments only), its approximate size in term of number of individuals, the number of individuals sampled (No.), the number of alleles A (adjusted for a sample size of 30 individuals using Ewens 1972's sampling formula), the gene diversity H_E, the observed heterozygosity H_O and the value of M statistics. The probability of rejecting the hypothesis of equilibrium in favour of a population size reduction (Bot P value) or expansion (Exp P value) was computed using the software BOTTLENECK (Piry *et al*. 1999) and assuming the SMM or the GSM (with a variance of 0.36) as mutation model.

microsatellite loci, that populations of the skink *Gnypetoscincus queenslandiae* are strongly structured with IBD patterns, due to restricted dispersal capabilities. In order to illustrate the IBD effects evidenced from our simulation data on a real biological system, we reanalysed the microsatellite data obtained by Sumner *et al*. (2004) on *G. queenslandiae* populations collected in recently fragmented and intact rainforest habitats. In this skink, the time-scaled density was estimated to be 50–192 individuals × generation/ha and dispersal rates to be 404–843 m^2/generation, hence resulting in small $D\sigma^2$ values between 3.82 and 14.6, with a point estimate of 5.5 (Sumner *et al*. 2001). The fragmentation of the studied habitats is known to have occurred 9–12 generations before sampling time, and fragmented populations remain isolated from the main continuous population (Sumner *et al*. 2004). In small forest fragments (F1 to F4, Table 2), skinks were sampled on the entire surface of the remnant rainforest fragment whereas larger fragments (F5 to F7, Table 2) and sites within the main continuous population (C1 to C5, Table 2) were sampled on an area of the size of the small fragments (see Table 2 for details about population and habitat sizes). This sampling strategy, at least for small fragments, corresponds to the large-scaled sampling strategy adopted in our simulation setting.

Because $D\sigma^2$ is 5.5 (point estimate) in *G. queenslandiae*, results from these skink populations have been compared with our simulation results obtained for $D\sigma^2 = 4$, the closest value in our parameter set. Table 2 shows that the numbers of alleles (8–9, Table 2) and the heterozygosity (0.62–0.70) in continuous sites are close to values obtained in our simulations for medium-size equilibrium populations (i.e. around 10 000–40 000 individuals). The number of alleles in the small rainforest fragments (F1 to F4 sites, Table 2) was significantly lower than in the continuous sites (7.48 vs. 8.43, respectively, for a sample size of 30 individuals; Mann–Whitney U-test: $Z = -2.45$, $P = 0.014$) and no significant difference was observed between large fragments (F5 to F7 sites, Table 2) and sites within the main continuous population (8.66 vs. 8.42, respectively; Mann-Withney U-test: $Z = -0.30$, $P = 0.77$). This is in agreement with our simulation results, which show that the decrease in the number of alleles in the first 20 generations after a habitat reduction under moderate IBD is substantial, and hence easily detectable only for small final habitat size (Fig. 3). No significant differences in heterozygosity (H_E or H_O) were detected between small or large fragments and sites within the main continuous population (Mann-Withney U-test: $Z = -0.25$, $P = 0.81$ and $Z = -1.4$, $P = 0.18$ in small fragments for H_E and H_O, respectively; $Z = -1.2$, $P = 0.23$ and $Z = -0.89$, $P = 0.37$ in large fragments for H_E and H_O, respectively). In agreement with this, our simulation results underlined the slower and hence hardly detectable loss of heterozygosity after recent habitat reduction, whatever the size of the final habitat (Fig. 4a, b).

Values of the statistics M (0.406–0.580, Table 2) were lower than the threshold value of 0.68 (Garza & Williamson 2001) in both fragmented and intact skink populations. Moreover, they were smaller in fragmented than in intact populations (mean M-values of 0.488 vs. 0.554, respectively; Mann-Withney U-test, $Z = -2.4$, $P = 0.018$). In agreement with

this, our simulations gave considerably lower values of M for IBD populations than in WF populations, those values often being lower than 0.68. Our simulations have also shown that for a moderate IBD structure (i.e. $D\sigma^2 = 4$) M-values are expected to be lower in nonequilibrium than in equilibrium IBD populations (Fig. 8a, b). Finally, the software BOTTLENECK did not detect any significant population size reduction signal in any skink population (Table 2). It rather detected significant deficits in heterozygosity (usually interpreted as expansion signals) for both fragmented and intact populations in 75% or 100% of the sites, depending on the assumed mutation model (GSM or SMM, respectively). In agreement with this, our simulations have shown the low power of the software BOTTLENECK to detect, with a limited number of microsatellite loci, recent population size reduction or habitat reduction events whatever the population model (Fig. 6a, b). Our simulations have also shown that IBD structure induces a high rate of false expansion signals, especially for scaled sampling strategy, large size populations at equilibrium or which have endured a recent reduction of habitat (Fig. 7).

Discussion

This study aimed at assessing the influence of spatially restricted dispersal (i.e. IBD) on several statistics summarizing within-population diversity at microsatellite loci, with a particular interest in finding signatures of habitat reduction on this diversity. We did not intend to propose new inferential methods for detecting habitat reduction from molecular markers in IBD populations, but rather explored how the comparative and single-point methods traditionally used in a WF population context behave for IBD populations. We found that a complex 'quartet' of factors was acting that include restricted dispersal, population size (i.e. habitat size), demographic history, and sampling scale. Despite this complexity, several strong and useful trends could be inferred from our simulation-based results.

Consequences of the spatial component of IBD models

In an IBD population at equilibrium, a local sample allows the estimation of local diversity (A and H_E), which may be considerably lower than the diversity in a sample including the same number of individuals but scaled to the entire habitat surface. On the one hand, when IBD is strong (i.e. for $\sigma^2 = 1/3$), A and H_E estimated from a local sample become roughly independent of the total population size and considerably lower than for WF populations of equivalent size (Fig. 2a, b). Scaling the sample to the entire habitat surface allows restoration of the positive correlation between A, H_E and population size, with values relatively similar to those estimated in a WF population. On the other hand, equilibrium IBD populations of small size (e.g. 400–1000 individuals), gave A and H_E values similar to those obtained for WF populations whatever the sampling scale, especially when dispersal was not too strongly limited in space.

H_O was roughly independent from the sampling scale (Fig. 2c). As a consequence, scaling the sample to the habitat surface did not restore the correlation between H_O and population size observed under a WF model for H_E and A (Fig. 2a, b). Dispersal restricted in space leads to a higher level of relatedness of breeding individuals and hence to offspring with a higher proportion of homozygous loci than under WF model, whatever the sampling scale and population size. H_O actually remained slightly lower in scaled samples than in local samples (Fig. 2c).To our mind, this can only be imputed to edge effects as reflective (or absorbing) boundaries simulated in this study induce smaller 'effective' population size on the edges of the population. Additional simulations in a completely homogeneous space such as a torus, showed no effect of sampling scale of H_O, confirming the edge effect of the boundaries for nontorus habitats (results not shown). We cannot exclude the possibility that border effects may to a certain extent influence other results in our study. Edge effects are likely to occur in real IBD population and would hence deserve further investigations.

We found that, after habitat size reduction, IBD populations are characterized by a higher inertia in the loss of genetic diversity (A, H_E and H_O) than WF populations (Figs 3 and 4). This inertia increases with the strength of IBD, and decreases when the sampling scale increases. Under a scaled sampling strategy, the rate of H_O loss, and to a lesser extent the rate of H_E loss, may be even higher in IBD than in WF populations for a recent reduction in population size. Hence, the IBD spatial effect seen in IBD equilibrium populations was further evidenced in nonequilibrium populations after habitat reduction. Local drift is slower at a local scale in IBD than in WF populations (see next section for theoretical insights), so that genetic diversity loss under IBD is delayed when measured at a small geographical scale.

Comparison with previous theoretical studies

Comparison of our simulation-based results with previous analytical or simulation studies of continuous IBD populations is limited by: (i) the differences in the mutational and demographic models, and (ii) the fact that all previous studies focused on the observed heterozygosity (H_O) as the statistic summarizing genetic diversity. However, several of our simulation-based results on H_O can be paralleled with previous theoretical studies.

We found that for small population sizes/surfaces, limited dispersal has a weak effect on the spatial genetic pattern, so that such populations could be considered as virtually evolving as WF populations. Several previous theoretical studies went further in this direction by concluding that most IBD populations can be regarded, independently of the

population surface, as randomly mating populations unless dispersal is strongly restricted in space (i.e. for $D\sigma^2 < 1$ in a population on a torus; Malécot 1948; Wright 1951; Maruyama 1972; for $D\sigma^2 < 2$ in a plane rectangular population; Maruyama 1972). Our simulation results for plan-squared populations are hence only partly congruent with these previous results, since we found that even an IBD structure with $D\sigma^2 = 4$ has a substantial influence on microsatellite genetic variability, when measured with different summary statistics (including H_O) and at different sampling scales. Those discrepancies might be due to the presence of mutations in our model and to differences in the demographic models considered such as differences in dispersal distributions and edge effects. Moreover, close examination of Maruyama (1972)'s analytical results shows that the used numerical approximations are not valid for $D\sigma^2$ values around the critical value of 2 for a plane population. Our simulation results are in better agreement with those of Kawata (1995) which show that the rate of decrease of H_O in a two-dimensional population on a continuous plane is different from that in a panmictic unit, unless $D\sigma^2$ is much greater than 1 (e.g. approximately 8).

Barton & Wilson (1995) have shown that the short-term rate of decrease of H_O in a population with Gaussian dispersal is given by $1/8t\pi D\sigma^2$ (compared to $1/N_T$ for a WF population of N_T genes), where t is the number of generations. The genetic diversity is thus expected to decrease faster under IBD than in WF population in the first generations for sufficiently large population size (i.e. for $N_T >> 8\pi D\sigma^2$), which is in agreement with our simulations for recent habitat reductions (e.g. 20 generations). For longer evolutionary times, Rousset (2004) has shown that, for an IBD population represented on a torus, the expected rate of decrease for H_O in the whole population is $(1 - F_{ST})/N_T$, where N_T is the total number of genes in the population and F_{ST} is calculated on the entire population considering each individual as a deme. Because a decrease in dispersal will increase F_{ST} values, limited dispersal is expected to retard the rate of decrease for H_O when compared to a WF population where the loss of genetic variation is $1/N_T$. Numerical approximations for the rate of decrease of H_O in a plane rectangular habitat derived by Maruyama (1972) suggest that for strong IBD structure, the rate of decrease of H_O can be approximated by $D\sigma^2/4N_T$, leading to similar conclusions.

We found a good agreement between Rousset's expectation on the rate of decrease of H_O and our simulation results for a scaled sample and not too recent habitat reductions (i.e. > 20 generations, results not shown). We also found that under a stepping-stone model (i.e. with $\sigma^2 = 1/3$), the rate of decrease in H_O was in close agreement with the rate of $D\sigma^2/4N$ given by Maruyama's approximations (results not shown). However, those agreements did not hold for smaller population sizes (i.e. < 400 individuals after habitat reduction; results not shown), probably because in small populations, edge effects are important and IBD structure is not rigorously described by $D\sigma^2$ alone (Rousset 1997). Again, the discrepancies observed between Maruyama's, Rousset's and our results might also be due to differences in the studied models (especially the presence of mutations in our model and different dispersal distributions). The multiplicity of the factors acting significantly on the pattern of polymorphism in both equilibrium and nonequilibrium IBD populations (sampling scale, dispersal distribution, habitat geometry including edge effects, demographic history, statistics used to summarize genetic diversity …) makes it difficult to describe this pattern using general analytical approximations, and hence gives weight to simulation-based study such as the present one.

Detecting habitat reduction in IBD populations

Our study shows that ignoring IBD structure leads in numerous cases to incorrect inferences about population demographic history, and hence stresses the need for empirical studies to better evaluate the magnitude of IBD in the sampled population. If IBD exits in the sampled population, sampling should be refined with a particular focus on the spatial scale relative to the entire population surface and on genetic or demographic estimation of $D\sigma^2$. Such information should help in interpreting the genetic patterns observed at molecular markers. Although our simulations indicate that there is no generic method to handle IBD data, several of our results should be of practical interest when aiming to detect habitat reduction.

First, we found that for a comparative approach, a scaled sample instead of a local sample reveals larger differences in genetic diversity statistics between equilibrium and size-reduced IBD populations. Hence, if one wants to test for a loss of genetic diversity due to habitat reduction using a comparative approach, large-scale sampling is preferred. However, it is worth noting here that a similar sampling scale should be applied in the compared IBD populations.

Second, the single-point approach of Cornuet & Luikart (1996) has shown relatively similar performances for IBD and WF populations. This is in agreement with our finding that allelic diversity is lost more quickly than heterozygosity after a population size reduction in both IBD and WF populations (Figs 3 and 4). Although some differences were observed in the loss of H_E and A between the two population models, it seems that such differences do not translate strongly in terms of ΔH values. One misleading bias has been detected for equilibrium situations and recent habitat reduction, however, since heterozygosity deficits and hence false expansion signals were more often detected in IBD than in WF populations (e.g. Fig. 7 and results from the skink population data of Sumner *et al*. 2004). Moreover, we found that a large-scaled sample reduced the proportion of detected population size reductions and increased the rate of

false expansion signals, suggesting that local samples should be used preferentially for the single-point approach of Cornuet & Luikart (1996). The risk of detecting false signal of expansion in equilibrium populations due to fine-scale population structure and large sampling scale has been previously stressed by Ptak & Przeworski (2002) in the context of sequence data analysis based on the Tajima's *D* statistics.

The method based on the statistic *M* was found to be strongly affected by departure from the underlying assumption of WF population (Fig. 8 and results on the skink population data of Sumner *et al*. 2004). Both equilibrium and post habitat reduction *M*-values were strongly dependent on the strength of IBD, and this occurred whatever the sampling scale. The detection of habitat reduction using the simulation-based critical value, proposed by Garza & Williamson (2001), hence appears particularly misleading for IBD populations. Besides the problem of determining a critical value that would make sense under IBD modalities, post-habitat reduction *M*-values remained lower than equilibrium values during a shorter time window in IBD than in WF populations, and then became larger (quickly in some cases) than initial equilibrium values.

We did not explore all available methods for the detection of demographic declines. In particular, maximum likelihood methods based on the coalescence theory and MCMC approaches has been recently developed (e.g. Kuhner *et al*. 1998; Beaumont 1999); these methods also assume a WF population model. Because such methods are computer-intensive and thus highly time-consuming, their behaviour could not be investigated in a spatially explicit context of habitat reduction. At first sight, it may appear more satisfying to develop *ad hoc* inferential tools for detecting population size reduction for IBD population, rather than testing for bias induced by departure from the WF model. However, besides the numerical difficulties of including IBD in a coalescent approach, a realistic parameterization of dispersal distributions remains challenging (Rousset 2004). We hence believe that a better solution would be to develop methods that are robust with regards to dispersal modalities. However, so far no satisfying approach has been proposed in this direction.

Acknowledgements

We thank Joanna Sumner for providing microsatellite data of *Gnypetoscincus queenslandiae*, Craig Moritz for constructive comments on the manuscript and François Rousset for useful discussions. This work was financially supported by a grant to A.E. and R.S. from the INRA research department Santé des Plantes et Environnement.

References

Barton NH, Wilson I (1995) Genealogies and geography. *Philosophical Transactions of the Royal Society of London. Series B, Biological Sciences*, **349**, 49–59.

Beaumont MA (1999) Detecting population expansion and decline using microsatellites. *Genetics*, **153**, 2013–2029.

Beaumont MA (2004) Recent developments in genetic data analysis, what can they tell us about human demographic history? *Heredity*, **92**, 365–379.

Cornuet JM, Luikart G (1996) Description and power analysis of two tests for detecting recent population bottlenecks from allele frequency data. *Genetics*, **144**, 2001–2014.

Crawford TJ (1984) The estimation of neighbourhood parameters for plant populations. *Heredity*, **52**, 273–283.

Crow JF, Kimura M (1970) *An Introduction to Population Genetics Theory*. Harper & Row, New York.

Diamond J (1989) Overview of recent extinctions. In: *Conservation for the Twenty-First Century* (eds Pearl M, Western D), pp. 37–41. Oxford University Press, New York.

Dudash MR, Fenster CB (2000) Inbreeding and outbreeding depression in fragmented populations. In: *Genetics, Demography and Viability of Fragmented Populations* (eds Young AG, Clarke GM), pp. 33–53. Cambridge University Press, Cambridge.

Dunham J, Peacock M, Tracy RC, Nielsen J, Vinyard G (1999) Assessing extinction risk: integrating genetic information. *Conservation Ecology* [online], **3**.

Ellegren H (2000) Heterogeneous mutation processes in human microsatellite DNA sequences. *Nature Genetics*, **24**, 400–402.

Endler JA (1977) *Geographical Variation, Speciation, and Clines*. Princeton University Press, Princeton, New Jersey.

Estoup A, Angers B (1998) Microsatellites and minisatellites for molecular ecology: theoretical and empirical considerations. In: *Advances in Molecular Ecology* (ed. Carvalho G), pp. 55–86. IOS Press, Amsterdam.

Estoup A, Wilson IJ, Sullivan C, Cornuet JM, Moritz C (2001) Inferring population history from microsatellite and enzyme data in serially introduced cane toads, *Bufo marinus*. *Genetics*, **159**, 1671–1687.

Ewens WJ (1972) The sampling theory of selectively neutral alleles. *Theoretical Population Biology*, **3**, 87–112.

Fahrig L (2003) Effects of habitat fragmentation on biodiversity. *Annual Review of Ecology, Evolution and Systematics*, **34**, 487–515.

Fenster CB, Vekemans X, Hardy OJ (2003) Quantifying gene flow from spatial genetic structure data in a metapopulation of *Chamaecrista fasciculata* (Leguminosae). *Evolution*, **57**, 995–1007.

Fisher RA (1921) On the mathematical foundations of theoretical statistics. *Philosophical Transactions of the Royal Society of London. Series A, Mathematical, Physical and Engineering Sciences*, **222**, 309–368.

Frankel OH, Soulé ME (1981) *Conservation and Evolution*. Cambridge University Press, Cambridge, UK.

Gaines MS, Diffendorfer JE, Tamarin RH, Whittam TS (1997) The effects of habitat fragmentation on the genetic structure of small mammal populations. *Journal of Heredity*, **88**, 294–304.

Garza JC, Williamson EG (2001) Detection of reduction in population size using data from microsatellite loci. *Molecular Ecology*, **10**, 305–318.

Goldstein DB, Harvey PH (1999) Evolutionary inference from genomic data. *Bioessays*, **21**, 148–156.

Goldstein DB, Roemer GW, Smith DA *et al.* (1999) The use of microsatellite variation to infer population structure and demographic history in a natural model system. *Genetics*, **151**, 797–801.

Griffiths RC, Tavaré S (1994) Sampling theory for neutral alleles in

a varying environment. *Philosophical Transactions of the Royal Society of London. Series B, Biological Sciences*, **344**, 403–410.

Guinand B, Scribner KT (2003) Evaluation of methodology for detection of genetic bottlenecks, inferences from temporally replicated lake trout populations. *Comptes Rendus Biologies*, **326**, S61–S67.

Hedrick PW, Kalinowski ST (2000) Inbreeding depression in conservation biology. *Annual Review of Ecology and Systematics*, **31**, 139–162.

Hurt C, Hedrick P (2004) Conservation genetics in aquatic species: general approaches and case studies in fishes and springsnails of arid lands. *Aquatic Sciences*, **66**, 402–413.

Kawata M (1995) Effective population size in a continuously distributed population. *Evolution*, **49**, 1046–1054.

Kingman JFC (1982a) The coalescent. *Stochastic Processes and Their Applications*, **13**, 235–248.

Kingman JFC (1982b) On the genealogy of large populations. *Journal of Applied Probabilities*, **19A**, 27–43.

Kot M, Lewis MA, Driessche PVD (1996) Dispersal data and the spread of invading organisms. *Ecology*, **77**, 2027–2042.

Kuhner MK, Yamato J, Felsenstein J (1998) Maximum likelihood estimation of population growth rates based on the coalescent. *Genetics*, **149**, 429–434.

Lacy RC, Lindenmayer DB (1995) A simulation study of the impacts of population subdivision on the mountain brushtail possum *Trichosurus caninus* Ogilby (Phalangeridae, Marsupialia), in south-eastern Australia. II. Loss of genetic variation within and between subpopulations. *Biological Conservation*, **73**, 131–142.

Lande R (1988) Genetics and demography in Biological Conservation. *Science*, **241**, 1455–1460.

Leblois R, Estoup A, Rousset F (2003) Influence of mutational and sampling factors on the estimation of demographic parameters in a 'continuous' population under isolation by distance. *Molecular Biology and Evolution*, **20**, 491–502.

Leblois R, Rousset F, Estoup A (2004) Influence of spatial and temporal heterogeneities on the estimation of demographic parameters in a continuous population using individual microsatellite data. *Genetics*, **166**, 1081–1092.

Luikart G, Cornuet JM (1998) Empirical evaluation of a test for identifying recently bottlenecked populations from allele frequency data. *Conservation Biology*, **12**, 228–237.

Malécot G (1948) *Les mathématiques de l'hérédité*. Masson, Paris.

Malécot G (1975) Heterozygosity and relationship in regularly subdivided populations. *Theoretical Population Biology*, **8**, 212–241.

Maruyama T (1972) Rate of decrease of genetic variability in a two-dimensional continuous population of finite size. *Genetics*, **70**, 639–651.

McGlaughlin M, Karoly K, Kaye T (2002) Genetic variation and its relationship to population size in reintroduced populations of pink sand verbena, *Abronia umbellata* subsp *breviflora* (Nyctaginaceae). *Conservation Genetics*, **3**, 411–420.

Miller CR, Waits LP (2003) The history of effective population size and genetic diversity in the Yellowstone grizzly (*Ursus arctos*): implications for conservation. *Proceedings of the National Academy of Sciences, USA*, **100**, 4334–4339.

Nei M (1987) *Molecular Evolutionary Genetics*. Columbia University Press, New York.

Nei M, Maruyama T, Chakraborty R (1975) Bottleneck effect and genetic variability in populations. *Evolution*, **29**, 1–10.

Nordborg M (2001) Coalescent theory. In: *Handbook of Statistical Genetics* (eds Sons JW, Balding DA, Bishop M, Cannings C). Chichester, UK.

Ohta T, Kimura M (1973) A model of mutation appropriate to estimate the number of electrophoretically detectable alleles in a finite population. *Genetical Research*, **22**, 201–204.

Oostermeijer JGB, Luijten SH, den Nijs JCM (2003) Integrating demographic and genetic approaches in plant conservation. *Biological Conservation*, **113**, 389–398.

Pannell JR (2003) Coalescence in a Metapopulation with recurrent local extinctions and recolonizations. *Evolution*, **57**, 949–961.

Piry S, Luikart G, Cornuet JM (1999) BOTTLENECK, a computer program for detecting recent reductions in the effective population size using allele frequency data. *Journal of Heredity*, **90**, 502–503.

Pritchard JK, Seielstad MT, Perez-Lezaun A, Feldman MW (1999) Population growth of human Y chromosomes, a study of Y chromosome microsatellites. *Molecular Biology and Evolution*, **16**, 1791–1798.

Ptak SF, Przeworski M (2002) Evidence for population growth in humans is confounded by fine-scale population structure. *Trends in Genetics*, **18**, 559–563.

Queney G, Ferrand N, Marchandeau S *et al.* (2000) Absence of a genetic bottleneck in a wild rabbit (*Oryctolagus cuniculus*). *Molecular Ecology*, **9**, 1253–1264.

Reich DE, Goldstein DB (1998) Genetic evidence for a Paleolithic human population expansion in Africa. *Proceedings of the National Academy of Sciences, USA*, **95**, 8119–8123.

Rousset F (1997) Genetic differentiation and estimation of gene flow from *F*-statistics under isolation by distance. *Genetics*, **145**, 1219–1228.

Rousset F (2000) Genetic differentiation between individuals. *Journal of Evolutionary Biology*, **13**, 58–62.

Rousset F (2004) *Genetic Structure and Selection in Subdivided Populations*. Princeton University Press, Princeton, New Jersey.

Saunders DA, Hobbs RJ, Margules CR (1991) Biological consequences of ecosystem fragmentation, a review. *Conservation Biology*, **5**, 18–32.

Schlotterer C (2000) Evolutionary dynamics of microsatellite DNA. *Chromosoma*, **109**, 365–371.

Spong G, Creel S (2001) Deriving dispersal distances from genetic data. *Proceedings of the Royal Society of London. Series B, Biological Sciences*, **268**, 2571–2574.

Stockwell CA, Hendry AP, Kinnison MT (2003) Contemporary evolution meets conservation biology. *Trends in Ecology & Evolution*, **18**, 94–101.

Sumner J, Jessop T, Paetkau D, Moritz C (2004) Limited effect of anthropogenic habitat fragmentation on molecular diversity in a rain forest skink, *Gnypetoscincus queenslandiae*. *Molecular Ecology*, **13**, 259–269.

Sumner J, Rousset F, Estoup A, Moritz C (2001) 'Neighbourhood' size, dispersal and density estimates in the prickly forest skink (*Gnypetoscincus queenslandiae*) using individual genetic and demographic methods. *Molecular Ecology*, **10**, 1917–1927.

Tajima F (1989) The Effect of Change in Population Size on DNA Polymorphism. *Genetics*, **123**, 597–601.

Vekemans X, Hardy OJ (2004) New insights from fine-scale spatial genetic structure analyses in plant populations. *Molecular Ecology*, **13**, 921–935.

Wayne RK, Morin PA (2004) Conservation genetics in the new molecular age. *Frontiers in Ecology and the Environment*, **2**, 89–97.

Wilkins JF (2004) A separation of timescales approach to the coalescent in a continuous population. *Genetics*, **168**, 2227–2244.

Williams BL, Brawn JD, Paige KN (2003) Landscape scale genetic effects of habitat fragmentation on a high gene flow species, *Speyeria idalia* (Nymphalidae). *Molecular Ecology*, **12**, 11–20.

Wright S (1931) Evolution in Mendelian populations. *Genetics*, **16**, 97–159.

Wright S (1943) Isolation by distance. *Genetics*, **28**, 114–138.

Wright S (1946) Isolation by distance under diverse systems of mating. *Genetics*, **31**, 39–59.

Wright S (1951) The genetical structure of populations. *Annals of Eugenics*, **15**, 323–354.

Young AC, Clarke GM (2000) *Genetics Demography and Viability of Fragmented Populations*. University Press, Cambridge, UK.